Scientific Research Publishing

International Journal of Geosciences, 2024, 15, 1113-1133
https://www.scirp.org/journal/ijg
ISSN Online: 2156-8367
ISSN Print: 2156-8359

Mineralogical and Geochemical Characterisation of Rocks and Geothermal Fluids in the Olkaria Geothermal Field, Kenya: Potential for Epithermal Deposits

Christine Jerotich Kiptoo[1], Isaac Kanda[2], Nicholas Mariita[1], Patrick Kariuki[1], Patrick Kirita Gevera[1,3]

[1]Geothermal Energy Training Institute (GeTRI), Dedan Kimathi University of Technology, Nyeri, Kenya
[2]Geothermal Development Company (GDC), Nakuru, Kenya
[3]Department of Civil Engineering, University of South Africa (Florida Science Campus), Johannesburg, South Africa
Email: kiptoochristine92@gmail.com

How to cite this paper: Kiptoo, C.J., Kanda, I., Mariita, N., Kariuki, P. and Gevera, P.K. (2024) Mineralogical and Geochemical Characterisation of Rocks and Geothermal Fluids in the Olkaria Geothermal Field, Kenya: Potential for Epithermal Deposits. *International Journal of Geosciences*, **15**, 1113-1133.
https://doi.org/10.4236/ijg.2024.1512058

Received: November 5, 2024
Accepted: December 27, 2024
Published: December 30, 2024

Abstract

The Kenyan Olkaria geothermal field has incredibly high geothermal potential in the East African Rift, the Kenyan Rift Valley. While the Olkaria geothermal area has been primarily attributed to electricity generation and direct uses, this research investigates the potential of epithermal deposits in the geothermal systems with particular interests in base metals (Zn, Pb, and Fe) and alkali metals (Li, Na, K) in geothermal rocks and fluids. The study employed geochemical, geological, and well-logging analyses to characterise and assess the conditions in the geothermal system suitable for forming and depositing epithermal minerals. Rock cuttings and fluid samples were collected from geothermal wells, fumaroles, and hot springs. Findings indicate that the mineralisation in the Olkaria wells occurs in microveins and disseminations in the rock matrix, majorly sulfides, and oxides in hydrothermal alteration zones. The reported Zn, Pb, and Fe mineralisation mainly relates to low sulphidation type from the characterised sulphur metal complexes and oxides. Fluid samples recorded the metals as follows: Fe (0.12 - 3.9 ppm), Zn (4.21 - 5.23 ppm), Pb (1.55 - 2.04 ppm), and lithium concentrations at ≤ 3 ppm, which is lower than extractible values in geothermal brines in the Salton Sea and geothermal fields of Europe. The economic characterisation of rocks and fluid samples in our area indicates that the concentration of base and alkali metals has not yielded economically viable values compared to other geothermal systems with economic grades. Detailed studies are recommended to quantify mineralisation in Olkaria geothermal fields and their extractability for sustainable management of the geothermal resource.

Keywords

East Africa Rift System (EARS), Epithermal Deposits, Geochemistry, Geothermal Systems

1. Introduction

With the rising climate change and global warming crisis, geothermal energy, among other clean energies, has been championed as one of the solutions to the issue by counteracting the overreliance on fossil fuels in the global industry since the 1880s [1]. Geothermal energy is renewable and has almost no carbon footprint in a closed system [2]. The East Africa Rift system has a geothermal potential of 15,000 MW, with the Kenyan Rift having an estimated potential of 10,000 MW, 944 MW being exploited at the geothermal areas shown in **Figure 1** [3] [4]. Geothermal exploitation in Kenya is mainly used for electricity generation, and other uses go towards recreational activities, such as fish farming, horticulture, and greenhouse heating [5] [6].

Some ancient and active geothermal systems have hydrothermal-epithermal deposits resulting from the movement of the high-temperature fluids, which precipitate upon conditions such as boiling and mixing fluids [7] [8]. Commonly reported metals in geothermal systems, including precious metals (gold, silver), base metals (Iron, zinc and lead), and Alkali metals (lithium, sodium and potassium), have been found in high concentrations in geothermal pipes and down-hole geothermal waters such as gold (180 ppm) and silver (8000 ppm) in the Ohaaki geothermal system in New Zealand [7] [9]. Other deposits have been recovered in the Hauraki goldfield with a production of 32,000 kg of gold and 1.5 Million kg of silver between the years 1862-2006 [10] and with a recent production of 6 metric tons of Au at Hishikari in 2021 [11].

Epithermal mineralisation forms in two characteristic environments: volcanic-hydrothermal systems and geothermal systems, based on the formation temperatures (<300˚C) and depth (<2 km), the mineralisation and sulfur fugacity [8] [12]. The epithermal deposits of the continental rifts are mostly low sulfidation deposits, with consideration given to the areas' magmatism, tectonic activities, and fluid chemistry.

To improve the economic potential of the Kenyan geothermal system beyond energy production, this paper reports on the objectives: mineralogical and chemical composition of well rock cuttings and geothermal fluids to establish the potential for critical minerals of economic value in the Olkaria geothermal area. We mainly report on the concentration of elements from wells, hot springs, and fumaroles and establish their economic potential for economic base metals exploration in the Olkaria geothermal system. Additionally, the alteration mineralogy in the wells cuttings is explored to determine formation conditions and economic viability of epithermal metal deposits.

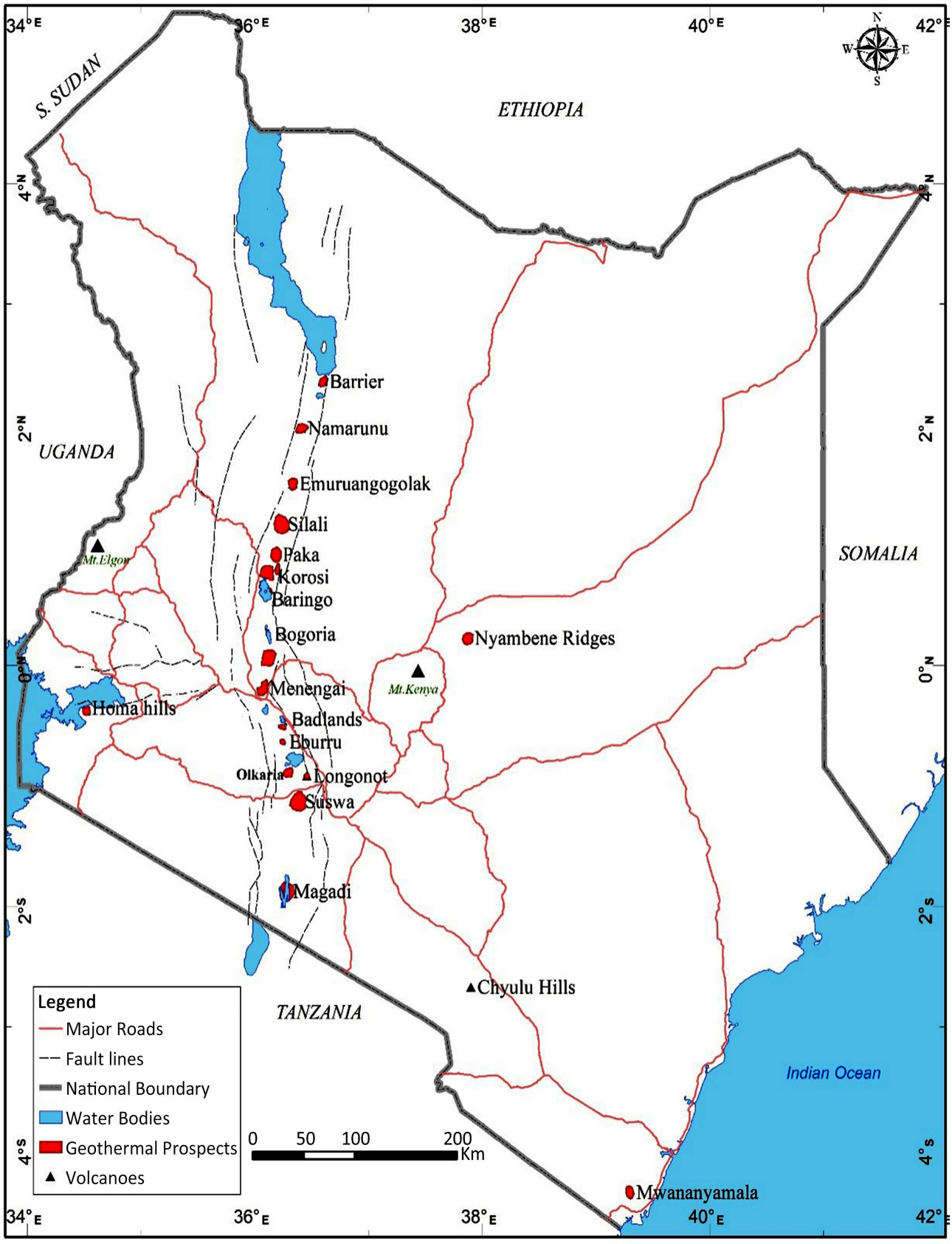

Figure 1. Geothermal areas/volcanic centers along the Kenyan rift valley with geothermal spots.

2. Materials and Methods

2.1. Geological and Tectonic Settings of Olkaria Geothermal area

The Olkaria geothermal complex is in the Kenyan segment of the East African Rift. This vast intra-continental extension structure runs from the northern Kenya-Lake Turkana to the northern Tanzania divergence. From earlier studies, the rift is presumed to have formed from the processes of mantle pluming and rifting events that led to the alkaline volcanism that characterises the rift to be bimodal-basalt-rhyolite rock types [13] [14]. The extension and evolution of the Kenyan rift have been revealed by radiometric dating to have begun in northern Kenya during the Oligocene-early Miocene times [14] [15]. This was preceded by volcanic activity in mid-Miocene 15 - 2 Ma [15]. The volcanism rendered the Kenyan rift to be predominantly covered by mafic lavas of the alkaline composition of transitional tholeiitic basalts and felsic lava of trachyte composition in the northern rift, trachyte and basalts occurrences in the south [14] [16].

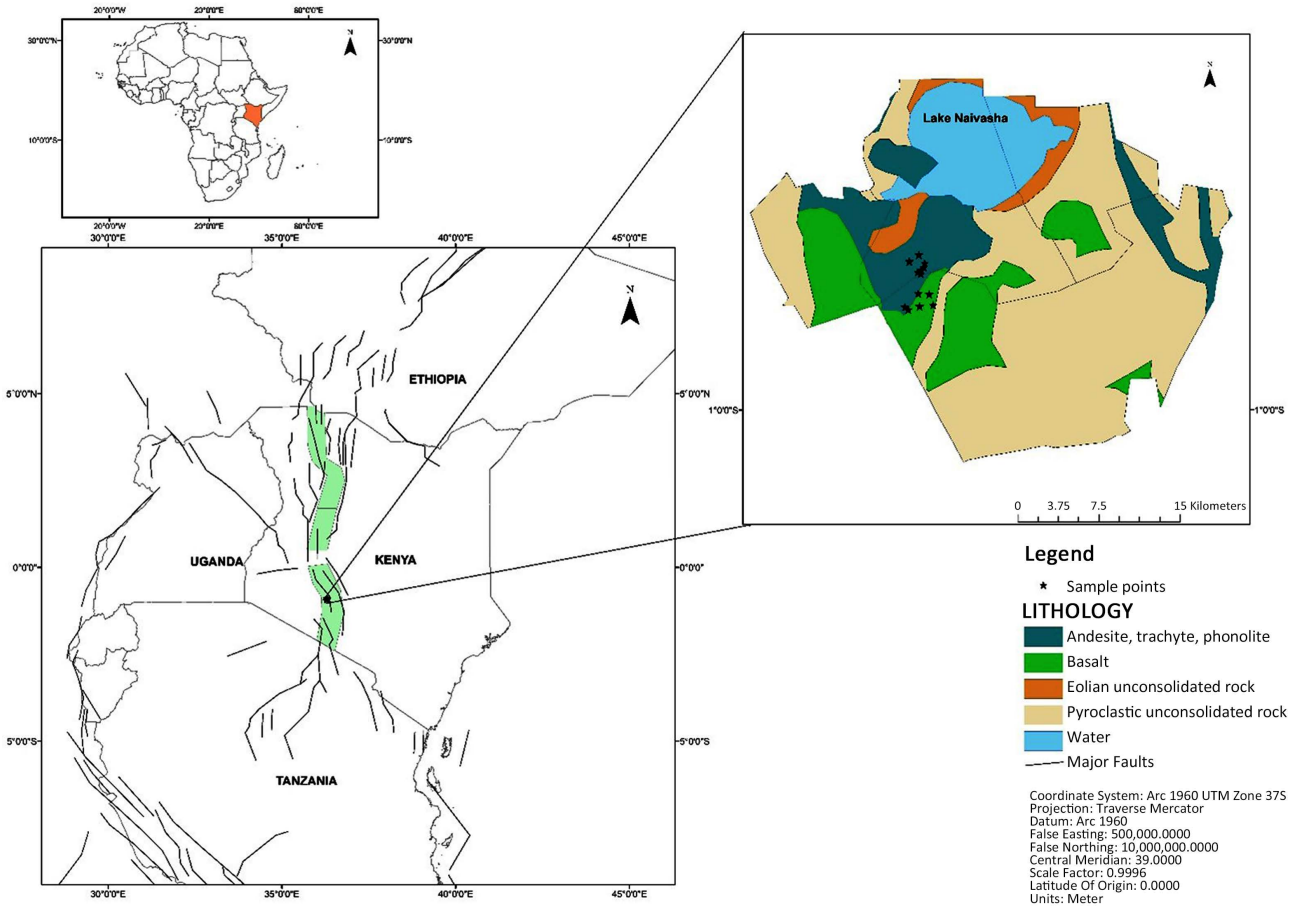

Figure 2. The local surface geology of the Olkaria geothermal volcanic complex.

The numerous Quaternary shield volcanoes formation rendered the Kenyan rift with many geothermal indicators such as hot springs, fumaroles, volcanic centres, solfatara, and hot-red grounds. The Olkaria geothermal complex is characterised by

numerous volcanic centres that have contributed to the vast success of exploring and exploiting geothermal energy in the area. The local geology of the study area, as seen in **Figure 2**, is characterised majorly by occurrences of comenditic rhyolites in the surface and the subsurface, intrusive rocks, basalts, pyroclastic and trachytes [17] [18].

2.2. Sample Collection

The samples were collected by KenGen, a geothermal development company in the Olkaria area. The samples collected include well rock cuttings, water from well discharge, hot springs, and fumaroles. The rock cuttings used were from three (3) geothermal wells: OW 802, OW 803, and OW 805. They were collected by the company's geologist during the geothermal well drilling processes from specific depths that showed sulfidation. The samples were then cleaned with water, dried, labelled, and stored for analysis. Fluids from the well discharge, hot spring, and fumaroles were collected in the Olkaria 1, southeast, and east fields. The samples were collected during the periodic well monitoring procedures where wells OW 802, OW 803, OW 805, OW 52, OW 52 A, OW 27, 31 &33, OW 32, and OW 35 were sampled in the Webre separator. The sampling of the fluids followed the guidance from the standard procedures [19] [20]. The aforementioned geothermal wells were logged for temperature and pressure.

2.3. Sample Preparation and Analysis

2.3.1. Petrographic Studies

Rock cuttings from the wells' cores were prepared into thin sections for petrographic microscopy. Binocular analysis was also conducted in the well logging site, where samples taken from a sample bag were placed in a petri dish and washed to remove impurities during drilling. The cuttings were then wetted to improve the visibility of features for the identification of sulfide dissemination. Stratigraphic sections from the petrographic reports were generated to highlight the lithology of the penetrated wells.

X-ray Diffractometer (XRD) was used to identify alteration minerals in the lithological units using the XRD-6000 SHIMADZU X-RAY diffractometer at the KenGen laboratories. Sample preparation was done using the standard procedure [21]. The rock cuttings were powdered and underwent three preparations: air-dried-untreated, glycolate-treated, and heated in the KenGen laboratory. The selected rock cuttings were analysed for hydrothermal alteration and clays. The petrographically analysed data were interpreted using the Logplot software version 8.

2.3.2. Fluid Geochemistry

The chemical composition of the fluid samples was analysed using Atomic Absorption Spectroscopy (AAS). The different water samples collected were examined for pH and temperature. They were also analysed for metals using AA-7000 Shimadzu Atomic Absorption Spectrometer (AAS) using the standard procedures outlined by Nicholson [19] using analytical grade calibration standards after every run as well as standard reference materials comprising of mass fractions and concentrations of the

eight metals (Fe, Zn, Mg, Mn, Pb, Li, Ca and Na). Anions (Cl-, SO_4, F–, CO_2^-) were examined using a Thermo Fisher scientific- UV-visible spectrophotometer evolution 201 and Ion-selective electrode_elit 20. These samples were prepared and analysed by the guide of the procedures used in the laboratory outlined by Nicholson [19]. The geochemical data were analysed using Excel software to correlate the amounts of the analysed metals, anions, and cations in the fluids. A piper plot graph in Excel was employed to characterise the water types in the Olkaria fields studied.

3. Results

3.1. Geothermal Well Stratigraphy

From the petrographic and well core results, the observed rock stratigraphic units in the three wells are as follows: rhyolites, comenditic rhyolites, trachytes, basalts, tuff, micro-granites and intrusions of syenitic, micro-granitic, basaltic and trachytic types. **Figure 3** and **Figure 4** indicate the stratigraphic rock units noted in the wells OW 802, OW 803, and OW 805.

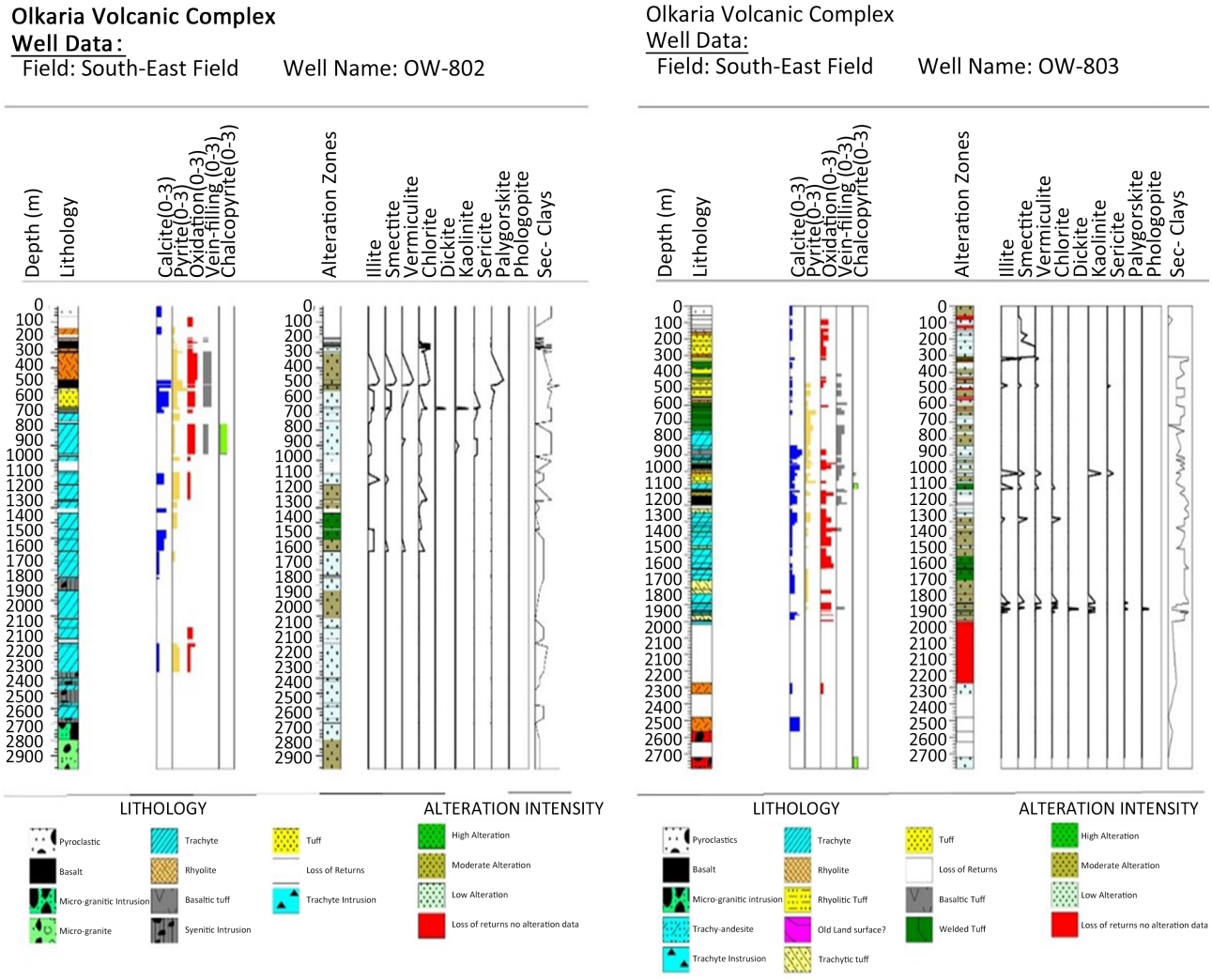

Figure 3. OW 802 and OW 803 stratigraphic, lithological sections, permeability indicator minerals, alterations, and alteration zones.

Wells (Figure 3 and Figure 4) are covered by pyroclastic in the uppermost rock unit. The rock is greyish-brown with loose fragments. It contains soils, clays, quartz, tuffs, volcanic glass, pumice, and obsidian. It has a pelitic texture and moderate oxidation at 0 - 148 m depths. It is underlain by rhyolites, basalt, and tuff intercalations at depths of 18 - 670 m. The major rock unit in the three wells (Figure 3 and Figure 4) is trachytes, observed at 650 - 2650 m depths. Well-formed euhedral sanidines, feldspars, and quartz at greater depths were noted at 1748 m and 2022 - 2024 m. The greater depths have intrusives with a high abundance of quartz and sanidine phenocrysts in the rock matrix and the high-temperature mineral indicator actinolite.

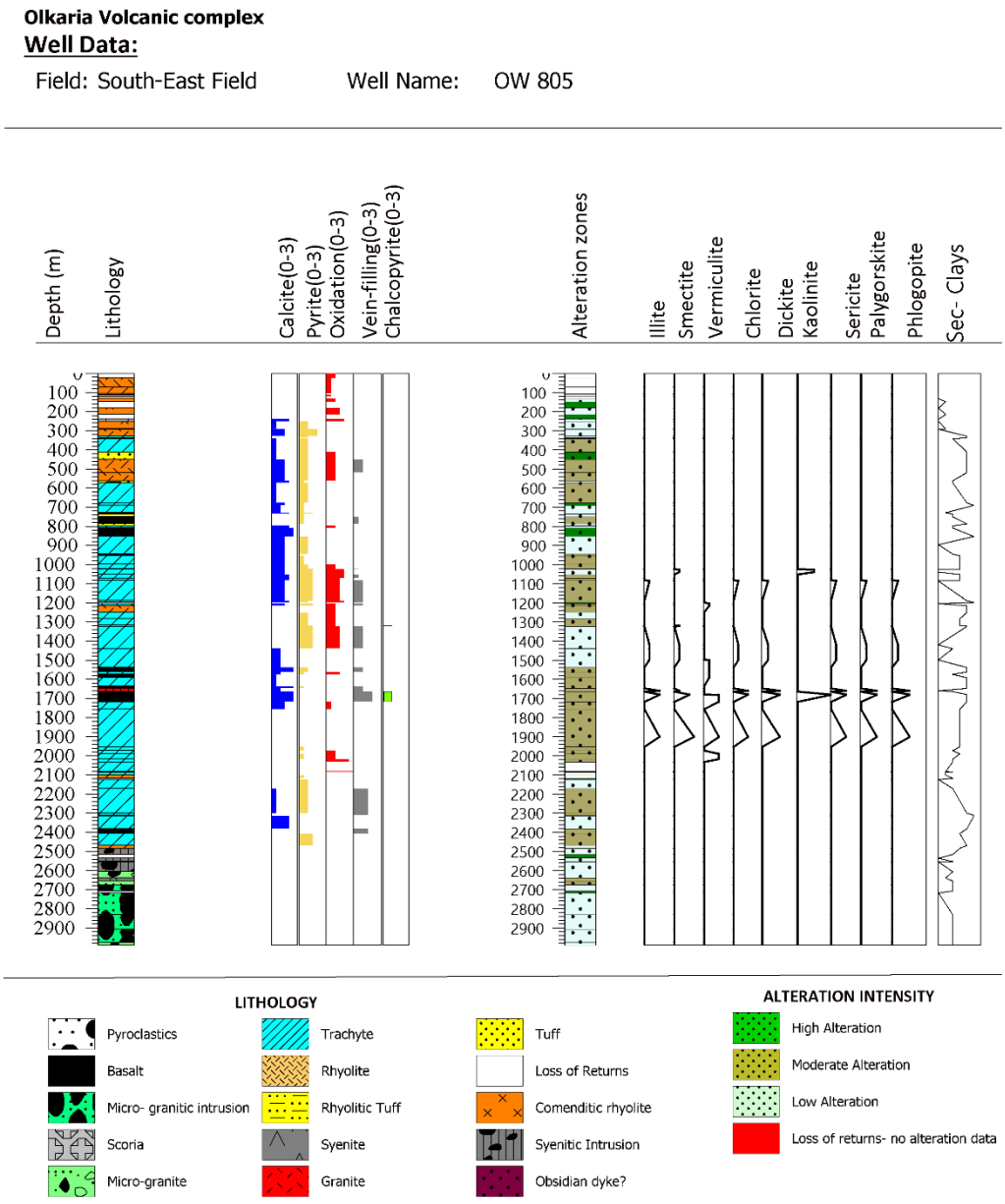

Figure 4. OW 805 Stratigraphic section, rock types, permeability indicator minerals, alterations, and alteration zones.

3.2 Secondary Mineralogy and Hydrothermal Alteration Minerals

From the petrographic studies and XRD analysis, the rock cuttings were noted to have a range of secondary-hydrothermal alteration minerals. These include oxides, sulfides, amorphous silica, sec-quartz, calcites, actinolite, wollastonite, wairakite and clays.

Table 1. A summary of the hydrothermal alteration minerals and the depth of their occurrence in the wells OW 802, OW 803, and OW 805.

Well ID / Hydrothermal alteration	OW 802	OW 803	OW 805
Illite	High occurrence 458 - 460 m, 618 - 858 m	High occurrence ≤ 500 m, 1010 - 1012 m. Minor at greater depths except at 1826 - 1828 m	Low sec clays ≤ 400 m, low-moderate 500 - 1650 m, 1898 - 1900 m
Smectite	High occurrence 458 - 460 m	Occurrence ≤ 500 m. present highly at 1010 - 1012 m	Low sec clays ≤ 400 m, low-moderate 500 - 1650 m. A high occurrence at 1898 - 1900 m
Chlorite	High occurrence 458 - 460 m	Minor	Minor occurrences 1898 - 1900 m
Vermiculite	High occurrence 458 - 460 m	Minor	Low sec clays ≤ 400 m, low-moderate 500 - 1650 m. High 1898 - 2000 m
Kaolinite	Minor ≥ 500 m	High ≥ 1010 - 1012 m, 1790 - 1792 m, low to moderate at ≥1798 m	Low sec clays ≤ 400 m, low-moderate 500 m - 1650 m. A high occurrence at 1658 - 1660 m
Sericite	Minor ≥ 500 m	Moderate-low 1010 - 1012 m	Minor
Dickite	Minor ≥ 500 m (700 - 600 m)	Moderate 1826 - 1828 m	Occurrence at 1084 - 1086 m.
Oxides	Low depths ≤ 500 m, 856 m - 858 m. Magnetite, Goethite, Ilmenite	Magnetite, Hematite minor at moderate-high depths, Hematite	Moderate-high at ≤ 500 m, Minor > 1000 m

Oxides: Oxides in the wells were noted in the near-surface depths, with siderite ranging from 100 - 500 m depths and 1790 - 1840 m (particularly in OW 803) in the three wells. Hematite is noted at lower depths of 138 m - 148 m, greater depths of 2074 - 2200 m in OW 802, and greater depths in OW 803 (1274 - 1322 m) and OW 805 (1214 - 1438 m). Magnetite is noted in well OW 803 only, at greater depths of 1790 - 1832 m, occurring with siderite at high oxidation and vein fillings.

Sulfides: Sulfides noted ranged from pyrite to chalcopyrite. Pyrite occurs along the wells in disseminations in the aphinitic rock matrix and is abundant at 500 m and 2406 - 2468 m. Chalcopyrite is not as pronounced as the pyrites in the well, with occurrences at greater depths in OW 802 (974 m), OW 803 (1072 - 1104 m) and OW 805 (1664 - 1716 m).

Silica: Quartz is notable in the samples along the wells, with mostly secondary quartz and amorphous silica, such as chalcedony, occurring < 500 m in the three wells. It is also noted at deeper depths of <1204 - 1214 m (OW 805) in micro veins and fractures.

Carbonates: Calcite in wells occurs intermittently along the wells, particularly in micro-veins and fractured basalts, rhyolitic tuffs, and trachytes. It is absent above 220 m in wells OW 802 and OW 805 and is noted to occur moderately at greater depths in OW 803, 2500 - 2600 m. Platy calcite in the wells is noted in greater depths of 1858 - 1862 m.

Clays: Clays were noted in wells primarily composed of illite, chlorite, smectite, kaolinite, and dickite alteration, as shown in diffractograms Figure 5 and Table 1. OW 802 and OW 803 have an abundance of smectite and chlorite <500 m and an increasing illite alteration with greater depths. Alteration clays in OW 805 are noted to be intense at 1678 - 1700 m, which also coincides with the minor deposits of metal Sulphide chalcopyrite and pyrite.

Clay alteration in OW 803 occurs at low depths between 316 - 480 m, with illite alteration and smectite clays occurring highly. Very low clays were detected between 500 - 1000 m, moderate to high illite, smectite, kaolinite, and sericite at 1010 - 1012 m and 1800 - 1828 m (Figure 3 and Table 1), similarly seen in OW 805.

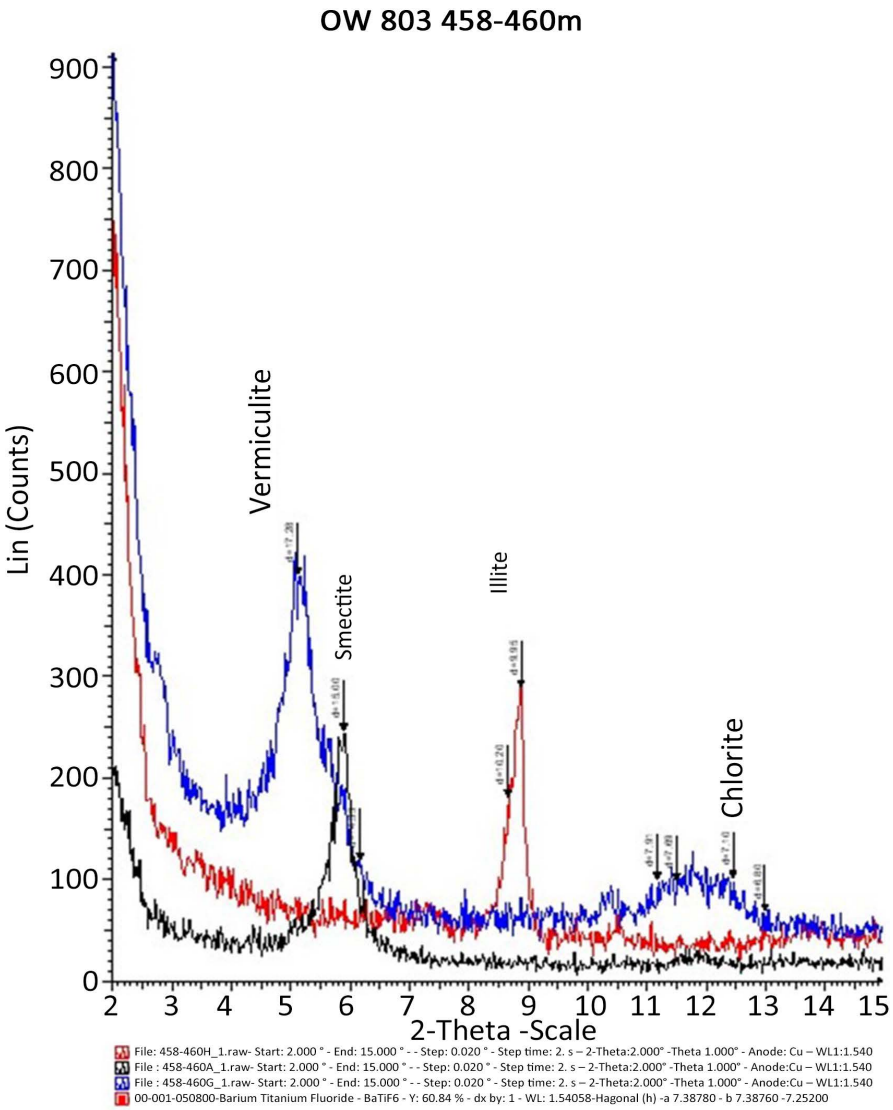

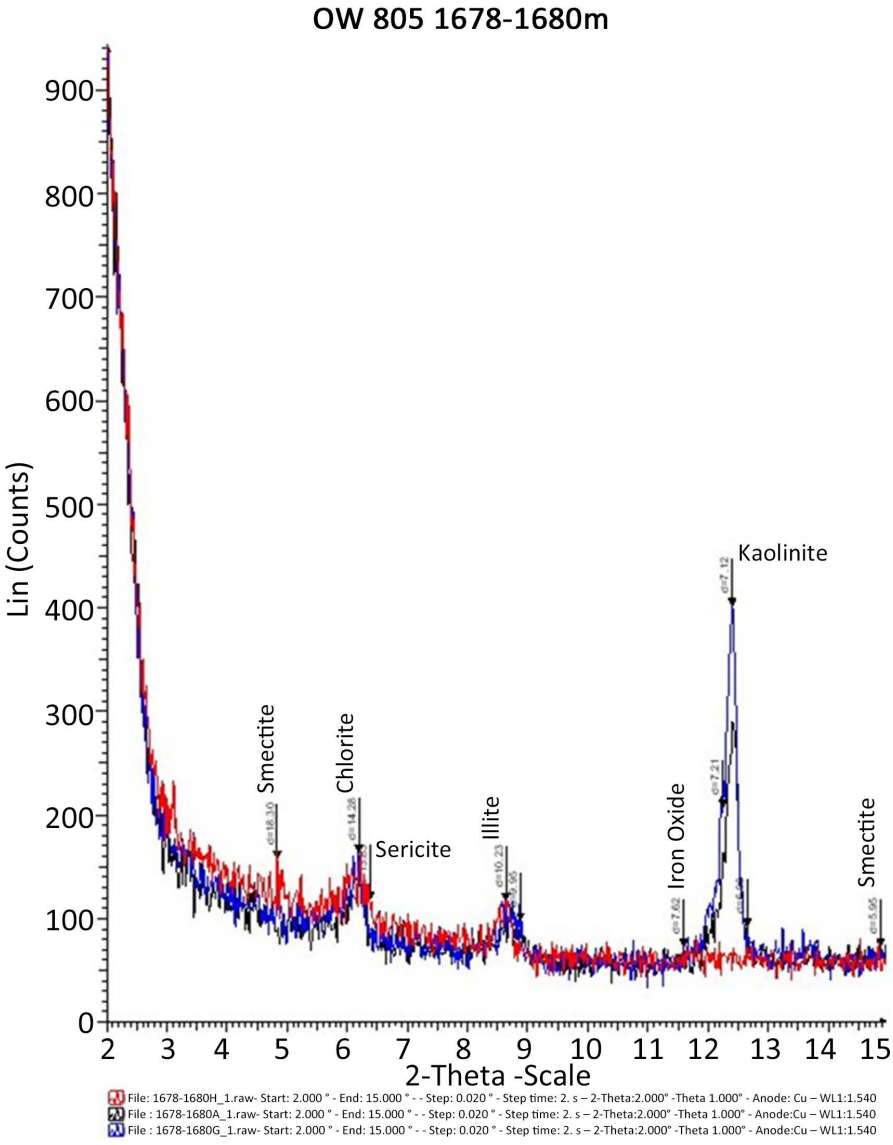

Figure 5. XRD patterns at different depths indicating alteration clays in the rock cuttings.

3.3 Fluid Geochemistry

The concentration of the metals in the fluid samples is indicated in the statistical estimation chemical data in **Table 2** and **Appendix A**. The statistical analysis of the distribution of the analysed fluid samples indicated the mean total dissolved solids (TDS) to be 2444.65 ppm, with OW52A having the highest amount of dissolved solids at 9730 ppm. The distribution of base metals and alkalis in the fluids varies in the samples in the study area. Fe concentration ranged from 0.12 ppm to 3.59 ppm, with a mean of 0.82 ppm and a standard deviation of 1.36 ppm. Its highest values are in hot springs and lowest in fumaroles (F4). The Zn concentration is high in OW52A and the lowest recorded value at OW 32, with a range value of 4.213 to 5.23 ppm, a mean value of 4.56 ppm, and a standard deviation of 0.48 ppm. Pb ranged from 1.55 ppm to 2.04 ppm, with a mean value of 1.765 ppm and

a standard deviation of 0.25 ppm. The highest values of Pb are noted in OW52A and the lowest at OW52. The alkali metals analysed in the samples recorded the highest Na, K, and Li values in wells OW 803, OW 52 A, and OW 52. Li concentration ranged from 0.001 - 3.09 ppm, with a mean of 1.52 and a standard deviation of 1.25 ppm. Na has the highest value of 2630.63 ppm at OW 52 A, and K is recorded highly at OW52 at 286.73 ppm.

Table 2. Fluid chemistry of Olkaria geothermal wells (OW-8 wells), fumaroles (F4&F5), and Hot spring (HS-2).

Parameters	Range	mean	Standard Deviation
Physical Parameters			
pH @20˚C	4.39 - 10.25	8.23	2.15
TDS (ppm)	14.3 - 9730	2444.65	2888.4
Chemical parameters (ppm)			
SO_4	5.07 - 322.96	98.59	101.37
Cl	4.69 - 3283.4	1031.63	1001.82
CO_2	31 - 579.0	283.79	184.86
F	0.04 - 533.4	129.38	157.83
Ca	0.0 - 2.40	0.61	0.85
Na	1.34 - 2630.63	816.35	761.68
K	0.20 - 286.734	141.17	142.73
Mg	0.0 - 0.5	0.09	0.17
Fe	0.12 - 3.59	0.82	1.36
Pb	1.55 - 2.04	1.765	0.25
Zn	4.213 - 5.23	4.56	0.48
Li	0.01 - 3.09	1.52	1.25

The geothermal waters from the southeast fields, fumaroles, hot springs, wells; OW 802, 803, and 805, and east field wells range in pH from 4.39 (F4) to 10.25 (OW 52A). The fumaroles are acidic, with an average of 4.4 pH, as seen in Appendix A. The cations and anions analysed in the fluids samples for water chemistry of the geothermal waters, as noted in Table 2 above, vary in concentration. High values noted are CO_2—579.0 ppm (F4), Cl—3283.4 ppm (OW 52A), SO_4—322.96 ppm (OW 52A), Ca—2.40 ppm (F4), and Mg—0.5 ppm (OW 35). The cations and anions are seen in the data table and analysed for water types shown in the Piper plot (Figure 6).

The dominant water type attributed to the reservoir, as seen in the piper plot shown in Figure 6, indicates calcium bicarbonate-rich water and sodium chloride

waters, particularly in all the sampled wells and spring 2, with the fumaroles exhibiting high bicarbonate in the fluids.

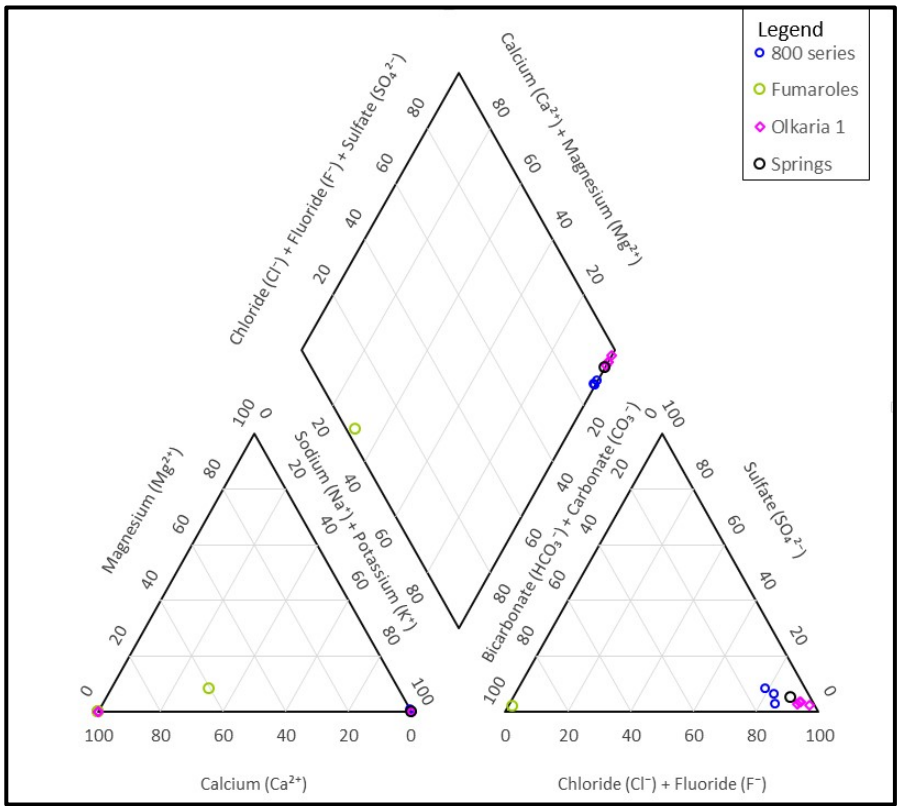

Figure 6. Water chemistry-type Piper plot of Olkaria wells, springs, and fumaroles.

3.4 Well Temperature Variation

The geothermal wells analysed for rock cuttings were logged to determine the temperature variation along the well. The actual well formation temperature of the wells after several well heat-up monitoring tests is shown in Figure 7, indicating the maximum temperature in the wells recorded is 297˚C. OW 802 well formation temperature varies from 186˚C at 100 m, increasing to the highest recorded temperature of 297.7˚C at 2800 m deeper in the well.

Well OW 803 formation temperature analysis indicates that the well ranges from the lowest recorded temperature of 72.8˚C at 100 m at the near-surface to 230˚C at 2400 m. Significant temperature variation in the well is between 500 - 900 m, from 86.8˚C to 191˚C. Formation temperature drops from 2450 m to 213˚C at 2950 m (final well depth). The variation of the well formation temperature in OW 805 shows a similarity to OW 803 graphically, with the lowest recorded temperature being at 100 m - 93.56˚C noted in Figure 7. There is an increase in temperature drastically from 500 m - 900 m with a leap from 94.07˚C - 206˚C. The highest recorded temperature is at a greater depth of 2350 m, being 276.37˚C, after which the temperature drops drastically to 237.3˚C at 2950 final well depth. This is probably a cold in the flow zone in the well, which is noted in

OW 803 as well (Figure 7).

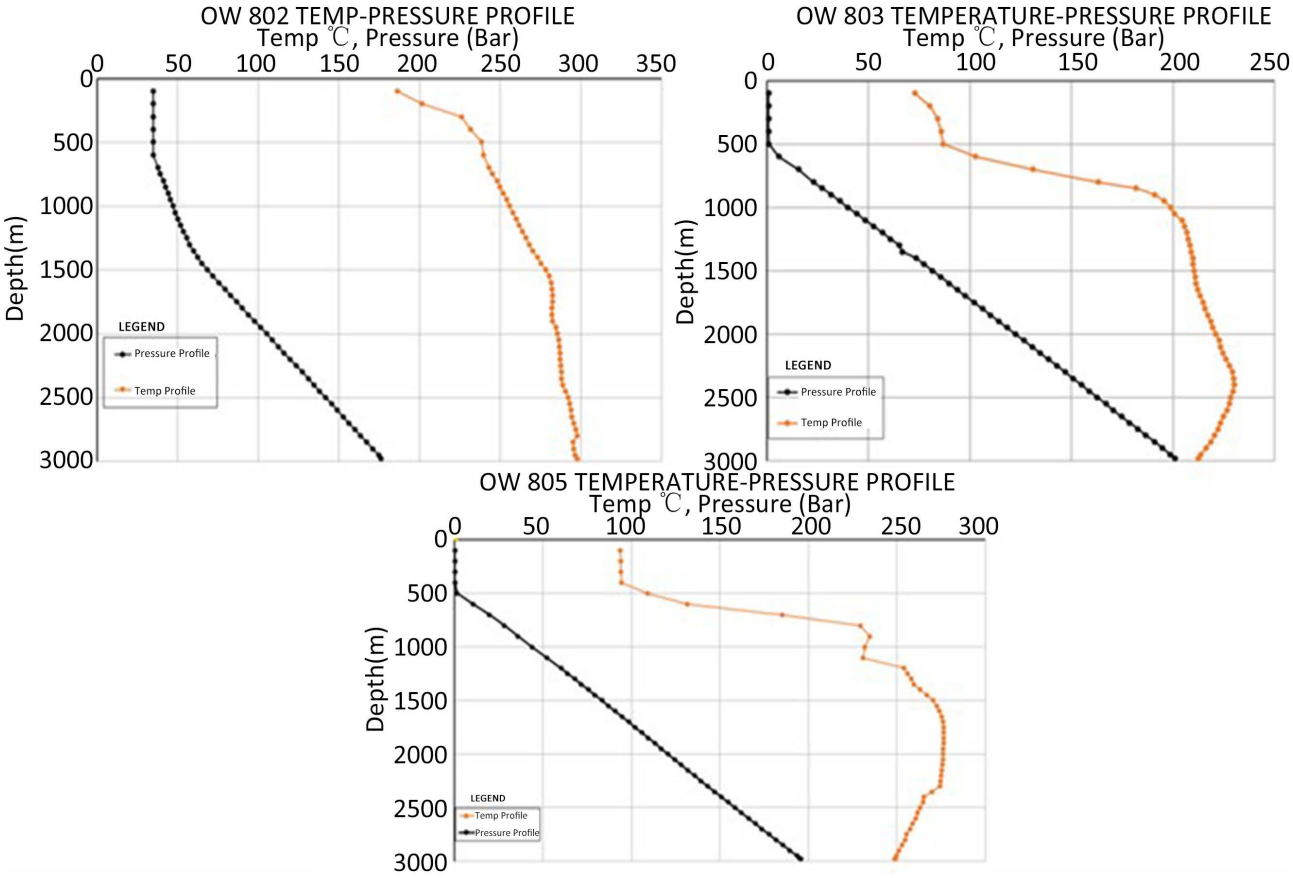

Figure 7. OW 802, OW 803, and OW 805 temperature-pressure profile log.

4. Discussion

The Olkaria geothermal complex has numerous volcanic centres with varying magmatic compositions, from trachytic and rhyolitic to basalt-related magma. The rock cuttings from the sampled wells range in composition, with the dominating rock unit being trachytes. The volcanic episodes in the area indicate periodic volcanism with intercalations between trachytic volcanism, basaltic, comenditic rhyolite, tuff, and pyroclastic eruptions, as noted in the well logs. Near-surface deposition of geothermal deposits in the Olkaria wells is seen to have occurrences of oxides and sulfides along the wells strata, with an abundance of oxides, clay alteration deposits, sulfides, and permeability indicator minerals such as adularia, and calcite, which agrees with research studies in Olkaria [18] [22].

The rock-water interaction in the subsurface aids in characterising the alteration types and mineralisation in the geothermal system. As heated geothermal fluids interact with rocks in the subsurface, they dissolve the minerals constituents in the rocks, which are transported with the fluids, upon which they are deposited when there is a mixing of fluids, boiling temperature, and or pressure conditions change in the conduit [7] [23]. The dissolved minerals depositions in our samples

are precipitates of minerals such as silica, calcite, and metal sulfides in microveins, fractures, and disseminations in the rock matrix. However, limited by the scope of the research, other geothermal systems have occurrences noted particularly in components such as wellheads scales of up to 25% ore forming minerals and pipes, hot springs, fumaroles, having some valuable concentrations of economic metal elements [24].

Oxides, mainly hematite, occur at lower depths in the wells, which may be attributed to the contribution of heated fluids mixing with colder fluids on the near-surface as seen by low-temperature variation (**Figure 7**), leading to oxidising conditions and deposition of secondary oxides [25]. The geothermal wells, in correlation to the sulfides, have notable pyrite and chalcopyrite, as seen in **Figure 3** and **Figure 4**. These indicate possible metal-sulfide complexing in these geothermal wells, particularly of low-range sulfidation noted in geothermal and hydrothermal systems studied for sulfidation-type deposits [8] [26]. Previous studies have indicated that numerous low sulfidation deposits, such as in Guanajuato, Batopilas, Fresnillo, Peru, New Zealand, and the United States such as Nevada, have been summarised to have sulfide assemblages typically sulfide-poor, dominated by pyrite [27]. The geochemical halos that are commonly distinctive from this system are mainly of illite or chlorite with major chloritization in mafic hosts [28]. We identified similar geochemical halos from the cuttings, indicating prominent illite and chloritization of the rhyolites, tuff, trachytes, and basalt. From hydrothermal minerals and clays in the rock cuttings, we identified that they are typically exhibiting silicic alteration at the near-surface < 500 m, characterised by the secondary minerals noted: silica, chalcedony, and quartz that are inferred to be from low-depth cooling water [26].

Observations at medium depths showed argillic-propylitic alteration, with illite + smectite + kaolinite + chlorite clays with oxides, pyrite, and calcite occurrences (**Figure 3** & **Figure 4**). At higher depths and temperatures of >220˚C, advanced argillic alteration characterises the wells with occurrences of kaolinite+ dickite, with illite, smectite, and chlorite as identified in the XRD clay patterns in **Figure 5**. The hydrothermal alteration phasing outwards from advanced argillic to argillic propylitic zones in the wells has notable deposits of sulfides and oxides. The significant sulfides in the Olkaria wells are pyrites which are noted to occur as vein fillings and disseminations in the rock matrix, a good indicator for permeable zones with precipitates which agrees with the previous studies in Olkaria [18], [29]-[32]. The alteration in the subsurface rocks of southeast fields of Olkaria wells is attributed to the Na-Cl rich, high alkalinity geothermal waters and brackish-saline waters > 1500 ppm based on Zakowski *et al.* [33].

A further look into the boiling zones in the wells indicated by the platy calcites coincides with the deposition of mineral deposits at depth, noted as argillic and advanced argillic alteration zones. Notable fracturing and vein filling at these permeable zones correspond with the high pyritisation and calcite depositions in OW 802. Considering the typical classification scheme for an epithermal system, the

Olkaria geothermal system is seen to have the sulfides species pyrite (deposited throughout the well) and minor chalcopyrite, classifying the geothermal system as a low sulfidation system [27] [34] [35].

Geochemistry of the Fluid Samples

The analysis for the major, trace, and alkali metals in the discharge samples has indicated a variable occurrence regarding the concentrations in the fluids (**Table 2**). Most transition metals in the geothermal fluids are generally low in our samples, indicating probable complexing into the secondary alteration minerals in the country rocks [36]. Hypersaline geothermal fluids in the Salton Sea US have high metal concentrations due to hydrothermal complexing with chlorides [37]. The studies in Olkaria geothermal fields have considered the mineral-fluid equilibrium to be a major controlling factor of the fluid composition in the system [38].

In the Olkaria geothermal area, economic metals analysed, such as lithium, range from <0.01 - 3.09 ppm, Zn from 4.28 - 5.2 ppm, and Fe from 0.12 - 3.59 ppm. From the comparison of our results with other geothermal systems like New Zealand and the Salton Sea, we could note a difference from the higher ranges recorded in these systems. The concentration range in these brines for Fe, Li, Zn, and Pb are <−0.1 - 0.25 ppm, 6.3 - 29 ppm, <−500 - 2295 ppb and 0.3 - 800 ppb, respectively [39]. The critical mineral lithium has been recorded in high values in brines of the geothermal fields of Europe, ranging between 125 - 450 mg/l, which is above or equal to what is considered economical for extraction of lithium: 150 mg/l [40]. A more practical and successful extraction of an economical grade, first kilogram lithium from geothermal brine was recently achieved in the Rhine Graben geothermal area with recorded concentration of 200 mg/l in the brine [41]. This project demonstrated the potential of taking advantage of economical grade critical minerals in geothermal brines from adsorption and ion exchange techniques applicable in any geothermal system with economical grade concentrations.

Lithium has also been recorded in the Roosevelt hot springs with values ranging between 20 - 30 mg/kg [42], which is in a similar range compared to the Salton Sea geothermal area in the United States of America. It has reported 400 mg/kg lithium in some brines, with other samples ranging from < 1 mg/kg to 20 mg/kg [37]. These are a closer range to some wells in Olkaria (<0.01 - 3.09 ppm), which is lower than those of economic grade. The metals have been seen to be of higher concentration in saline Na-Cl geothermal waters where the geothermal fluids have had intensive interaction with the rocks in the subsurface. Older geothermal systems may have had time to dissolve, concentrate, and precipitate elements, as noted in geothermal systems like the Okuaizu geothermal system in Japan, which dates back to the late Cenozoic volcanism [43]. The East African Rift system is comparatively younger, having developed in the Oligocene and is still active in this quaternary period. The elements in this younger system might need longer for water-rock interaction for economical mineral dissolution and precipitation.

The economical characterisation of the rocks and fluid samples in our area indicates that the concentration of base and alkali metals has not yielded economically viable values compared to other geothermal systems with economical grades of these metals.

The research has achieved its aim of looking into the potential of economic minerals base (Zn, Pb, and Fe) and alkali metals (Li, Na, K) in the Olkaria geothermal area. However, the study encountered some limitations which affected the scope of our findings. The main limitation included financial constraints, which affected our ability to analyse all the economic metals across the collected samples. This particular constraint narrowed down our focus to alkali and base metals discussed above. Hence, it potentially leaves out other valuable information that could be there on other economically significant minerals in the Olkaria geothermal system.

The research, however, identified the presence of mineralisation, particularly in the rock cutting cores, which are mostly the dissemination of pyrites, veins, and fracture filling with sulfides and calcites that indicated good permeability and precipitation of minerals in the subsurface. Higher deposition of metal sulfides has been mostly correlated to occur in zones of illite-smectite-chlorite alteration and also in advanced argillic alteration zones (Dickite-Kaolinite, Illite). The concentration ranges of the metals in fluid samples are <150 ppm, which are equally similar in values (apart from precious metals, which were not analysed due to funding constraints and laboratory limits), with some geothermal areas, as those discussed. However, the metals in fluid samples are not high enough for economical mining recommendations. Being a younger evolving rift with bimodal-trachyte-rhyolite basalt magma and rock composition, there could be longer water-rock interaction that could increase the concentrations in the fluids and depositions subsurface. The study, however, recommends additional research on the precipitates in the geothermal components, such as the geothermal pipes, wellheads, and control equipment that may harbour conditions such as sudden pressure-temperature drops that cause the precipitation of minerals. Their geochemical signatures would give more insight into the metal complexes in our geothermal fluids in Olkaria.

5. Conclusion

This research study was centred on identifying the epithermal deposits in the Olkaria geothermal system with a particular target at economic base metals (Zn, Pb, Fe) and alkali metals (Li, Na, K). The research objectives were to analyse the potential occurrence, the conditions, and the mineralisation of epithermal minerals and fluid metal concentrations in the Olkaria geothermal system. The results have indicated the achievement of objectives by identifying the lithological distribution in the geothermal wells, the mineralisation and hydrothermal alterations, the concentration of trace elements (Zn, Pb, Fe), and the alkali metals (Li, Na, K) in geothermal fluids samples from well discharges. The geothermal well cuttings in

Olkaria are dominated by trachyte rocks and dominating trachytic intrusion at depth with ranging fluid temperatures of 72.8˚C to 297˚C. The metal analysis in fluids shows that the dominant high-concentration elements are iron, zinc, sodium, and potassium. Lithium also has a higher concentration in fluids, mostly correlated to Na-Cl waters. The possible occurrence of the epithermal metal deposits in the Olkaria system indicates low sulfur species occurrence, limited to pyrite and chalcopyrite (minor amounts), hosted by the bimodal (trachyte-rhyolite basalt) rock assemblages. The metal sulfides occur as disseminations in the host rocks, and some pyrites are emplaced in micro-fracture and micro veins with hydrothermal clays at temperatures ranging from 225˚C - 270˚C. The metal deposits in the studied sectors of the Olkaria geothermal system are trace amounts and hence uneconomical compared with the Salton Sea, New Zealand Europe fields, and Hauraki geothermal systems with economical grade deposits of Li, Fe, Zn, and precious metals. However, more research could be done on the precipitates and fluid samples on the potential economical metals not analysed and amounts of critical metals, such as lithium metal, in other sectors of the Olkaria geothermal system.

Acknowledgements

The Authors acknowledge the Dedan Kimathi University of Technology for the research funding support and the Geothermal Training and Research Institute for their support in providing remarks and corrections in the paper, including tutorial fellows Dennis Njagi, Sophy Kipkowny, Purity Kamau and Mary Karanja. We also acknowledge the Kenya Electricity Generating Company (KenGen) for their support in accessing data for the research.

Source of Funding

The research was funded by Dedan Kimathi University of Technology under the Graduate Assistantship programme.

Authors' Contribution

The authors were involved in coming up with the design of the project. The research was funded by Dedan Kimathi University of Technology to Christine Kiptoo as an MSc Research grant. CK wrote the first draft of the research which was subsequently improved by CK, PG, IK, PK and NM. All authors have read and approved the submission of the manuscript.

Conflicts of Interest

The authors declare no conflicts of interest regarding the publication of this paper.

References

[1] Ritchie, H. and Rosado, P. (2020) Energy Mix. https://ourworldindata.org/energy-mix

[2] World Energy Council (2016) World Energy Resources 2016. 6-46.

[3] Omenda, P.A. (2014) The Geology and Geothermal Activity of the East African Rift. Short Course IX on Exploration for Geothermal Resources, Organized by UNU-GTP, GDC and KenGen, at Lake Bogoria and Lake Naivasha.

[4] Richter, A. (2023) Think Geo Energy's Top 10 Geothermal Countries 2022—Power Generation Capacity (MW). Think Geo Energy. https://www.thinkgeoenergy.com/thinkgeoenergys-top-10-geothermal-countries-2022-power-generation-capacity-mw/

[5] Lagat, J. (2010) Direct Utilization of Geothermal Resources in Kenya. *Proceedings World Geothermal Congress* 2010, Bali, 25-29 April 2010, 25-29.

[6] Mburu, M. (2022) Direct-Use of Geothermal Energy in Kenya. 1-13. https://www.grocentre.is/static/files/GTP/ShortCourses/Kenya/SC-30/0905directus-esgeothermalenergykenyamm3001.pdf

[7] Simmons, S.F. (2000) Hydrothermal Minerals and Precious Metals in the Broadlands-Ohaaki Geothermal System: Implications for Understanding Low-Sulfidation Epithermal Environments. *Economic Geology*, **95**, 971-999. https://doi.org/10.2113/95.5.971

[8] Dilles, J.H. and John, D.A. (2021) Porphyry and Epithermal Mineral Deposits. In: Alderton, D. and Elias, S.A., Eds., *Encyclopedia of Geology*, Elsevier, 847-866. https://doi.org/10.1016/b978-0-08-102908-4.00005-9

[9] Raymond, J., Williams-Jones, A.E. and Clark, J.R. (2005) Mineralization Associated with Scale and Altered Rock and Pipe Fragments from the Berlín Geothermal Field, El Salvador; Implications for Metal Transport in Natural Systems. *Journal of Volcanology and Geothermal Research*, **145**, 81-96. https://doi.org/10.1016/j.jvolgeores.2005.01.003

[10] Christie, A.B., Simpson, M.P., Brathwaite, R.L., Mauk, J.L. and Simmons, S.F. (2007) Epithermal Au-Ag and Related Deposits of the Hauraki Goldfield, Coromandel Volcanic Zone, New Zealand. *Economic Geology*, **102**, 785-816. https://doi.org/10.2113/gsecongeo.102.5.785

[11] Morishita, Y. and Yabe, Y. (2022) Genesis and Evolution of Hydrothermal Fluids in the Formation of the High-Grade Hishikari Gold Deposit: Carbon, Oxygen, and Sulfur Isotopic Evidence. *Minerals*, **12**, Article 1595. https://doi.org/10.3390/min12121595

[12] Lindgren, W. (1933) Mineral Deposits. McGraw-Hill Book Company.

[13] Baker, B.H., Mohr, P.A. and Williams, L.A.J. (1972) Geology of the Eastern Rift System of Africa. In: Baker, B.H., Mohr, P.A., and Williams, L.A.J., Eds., *Geological Society of America Special Papers*, Geological Society of America, 1-68. https://doi.org/10.1130/spe136-p1

[14] Furman, T. (2007) Geochemistry of East African Rift Basalts: An Overview. *Journal of African Earth Sciences*, **48**, 147-160. https://doi.org/10.1016/j.jafrearsci.2006.06.009

[15] Morley, C.K., Wescott, W.A., Stone, D.M., Harper, R.M., Wigger, S.T. and Karanja, F.M. (1992) Tectonic Evolution of the Northern Kenyan Rift. *Journal of the Geological Society*, **149**, 333-348. https://doi.org/10.1144/gsjgs.149.3.0333

[16] King, B.G., Chapman, G.R., Robson, D.A. and McConnell, R.B. (1972) Volcanism of the Kenya Rift Valley. *Philosophical Transactions of the Royal Society of London. Series A, Mathematical and Physical Sciences*, **271**, 185-208.

[17] Omenda, P.A. (1998) The Geology and Structural Controls of the Olkaria Geothermal

System, Kenya. *Geothermics*, **27**, 55-74. https://doi.org/10.1016/s0375-6505(97)00028-x

[18] Lagat, J., Arnorsson, S. and Franzson, H. (2005) Geology, Hydrothermal Alteration and Fluid Inclusion Studies of Olkaria Domes Geothermal Field, Kenya. *Proceedings World Geothermal Congress* 2005, Antalya, 24-29 April 2005, 24-29.

[19] Nicholson, K. (1993) Gas Chemistry. In: Nicholson, K., Ed., *Geothermal Fluids*, Springer Berlin Heidelberg, 87-115. https://doi.org/10.1007/978-3-642-77844-5_3

[20] Halldór Ármannsson, M.Ó. (2014) Geothermal Sampling and Analysis. Kenya Electricity Generating Co., Ltd., 1-8.

[21] Shen, S., Zaidi, S.R., Mutairi, B.A., Shehry, A.A., Sitepu, H., Hamoud, S.A., *et al.* (2012) Quantitative XRD Bulk and Clay Mineralogical Determination of Paleosol Sections of Unayzah and Basal Khuff Clastics in Saudi Arabia. *Powder Diffraction*, **27**, 126-130. https://doi.org/10.1017/s088571561200022x

[22] Mibei, G. (2012) Geology and Hydrothermal Alteration of Menengai Geothermal Field. Case Study: Wells Mw-04 And Mw-05. https://gogn.orkustofnun.is/unu-gtp-report/UNU-GTP-2012-21.pdf

[23] Ngothai, Y., Yanagisawa, N., Pring, A., Rose, P., Neill, B.O. and Brugger, J. (2010) Australian Geothermal Conference 2010 Mineral Scaling in Geothermal Fields: A Review Australian Geothermal Conference 2010. https://www.geothermal-energy.org/pdf/IGAstandard/AGEC/2010/Ngothai_et_al_2010.pdf

[24] Reyes, A.G., Trompetter, W.J., Britten, K. and Searle, J. (2003) Mineral Deposits in the Rotokawa Geothermal Pipelines, New Zealand. *Journal of Volcanology and Geothermal Research*, **119**, 215-239. https://doi.org/10.1016/s0377-0273(02)00355-4

[25] Stefánsson, A., Keller, N.S., Robin, J.G., Kaasalainen, H., Björnsdóttir, S., Pétursdóttir, S., *et al.* (2016) Quantifying Mixing, Boiling, Degassing, Oxidation and Reactivity of Thermal Waters at Vonarskard, Iceland. *Journal of Volcanology and Geothermal Research*, **309**, 53-62. https://doi.org/10.1016/j.jvolgeores.2015.10.014

[26] Hedenquist, J.W., Antonio Arribas, R. and Gonzalez-Urien, E. (2000) Exploration for Epithermal Gold Deposits. *Reviews in Economic Geology*, **13**, 245-277.

[27] Kissin, S.A. and Mango, H. (2014) Silver Vein Deposits. *Treatise on Geochemistry*, **13**, 425-432. https://doi.org/10.1016/b978-0-08-095975-7.01118-9

[28] Einaudi, M.T., Hedenquist, J.W. and Inan, E.E. (2003) Sulfidation State of Fluids in Active and Extinct Hydrothermal Systems: Transitions from Porphyry to Epithermal Environments. In: Simmons, S.F. and Graham, I., Eds., *Volcanic, Geothermal, and Ore-Forming Fluids: Rulers and Witnesses of Processes within the Earth*, Society of Economic Geologists, 285-313.

[29] Karingithi, C.W. (2000) Geochemical Characteristics of the Greater Olkaria Geothermal Field, Kenya. Report 9 in Geothermal Training in Iceland 2000. UNU-GTP, 165-188.

[30] Musonye, X.S. (2015) Sub-Surface Petrochemistry, Stratigraphy and Hydrothermal Alteration of the Domes Area, Olkaria Geothermal Field, Kenya. Master's Thesis, University of Iceland.

[31] Okoo, J., Omiti, A., Kamunya, K. and Saitet, D. (2017) Updated Conceptual Model of Olkaria Geothermal Field Naivasha, Kenya. *Transactions—Geothermal Resources Council*, **41**, 1536-1553.

[32] Kibet, M.K., Magut, P.K.S. and Varet, J. (2019) Rock Types and Alteration Mineralogy Occurring in Rock Types and Alteration Mineralogy Occurring in Olkaria Geo-

thermal Field. *IOSR Journal of Applied Geology and Geophysics*, **7**, 47-57.

[33] Zakowski, K., Narozny, M., Szocinski, M. and Darowicki, K. (2014) Influence of Water Salinity on Corrosion Risk—The Case of the Southern Baltic Sea Coast. *Environmental Monitoring and Assessment*, **186**, 4871-4879. https://doi.org/10.1007/s10661-014-3744-3

[34] Sillitoe, R.H. and Hedenquist, J.W. (2003) Linkages between Volcanotectonic Settings, Ore-Fluid Compositions, and Epithermal Precious Metal Deposits. In: Simmons, S.F. and Graham, I., Eds., *Volcanic, Geothermal, and Ore-Forming Fluids: Rulers and Witnesses of Processes within the Earth*, Society of Economic Geologists, 315-343.

[35] Pugliese, F.E., Pugliese, L.E., Dahlquist, J.A., Stipp Basei, M.A. and Martínez Dopico, C.I. (2021) Intermediate Sulfidation Epithermal Pb-Zn (± Ag ± Cu ± In) and Low Sulfidation Au (± Pb ± Ag ± Zn) Mineralization Styles in the Gonzalito Polymetallic Mining District, North Patagonian Massif. *Journal of South American Earth Sciences*, **110**, Article ID: 103388. https://doi.org/10.1016/j.jsames.2021.103388

[36] Kaasalainen, H., Stefánsson, A., Giroud, N. and Arnórsson, S. (2015) The Geochemistry of Trace Elements in Geothermal Fluids, Iceland. *Applied Geochemistry*, **62**, 207-223. https://doi.org/10.1016/j.apgeochem.2015.02.003

[37] Neupane, G. and Wendt, D.S. (2017) Assessment of Mineral Resources in Geothermal Brines in the US. *Proceedings* 42*nd Workshop on Geothermal Reservoir Engineering Stanford University*, Stanford, 13-15 February 2017,1-18.

[38] Wanyonyi, E.W. (2014) Fluid-Rock Interaction and Initial Aquifer Geochemistry in the Olkaria Geothermal System. https://rafhladan.is/bitstream/handle/10802/23984/UNU-GTP-2014-34.pdf?sequence=1

[39] Sajkowski, L., Turnbull, R. and Rogers, K. (2023) A Review of Critical Element Concentrations in High Enthalpy Geothermal Fluids in New Zealand. *Resources*, **12**, Article 68. https://doi.org/10.3390/resources12060068

[40] Sanjuan, B., Gourcerol, B., Millot, R., Rettenmaier, D., Jeandel, E. and Rombaut, A. (2022) Lithium-Rich Geothermal Brines in Europe: An Up-Date about Geochemical Characteristics and Implications for Potential Li Resources. *Geothermics*, **101**, Article ID: 102385. https://doi.org/10.1016/j.geothermics.2022.102385

[41] Kölbel, L., Kölbel, T., Herrmann, L., Kaymakci, E., Ghergut, I., Poirel, A., *et al.* (2023) Lithium Extraction from Geothermal Brines in the Upper Rhine Graben: A Case Study of Potential and Current State of the Art. *Hydrometallurgy*, **221**, Article ID: 106131. https://doi.org/10.1016/j.hydromet.2023.106131

[42] Simmons, S.F., Kirby, S., Verplanck, P. and Kelley, K. (2018) Strategic and Critical Elements in Produced Geothermal Fluids from Nevada and Utah. *Proceedings of* 43*rd Workshop on Geothermal Reservoir Engineering Stanford University*, Stanford, 12-14 February 2018.

[43] Mizugaki, K. (2000) Geologic Structure and Volcanic History of the Yanaizu-Nishiyama (Okuaizu) Geothermal Field, Northeast Japan. *Geothermics*, **29**, 233-256. https://doi.org/10.1016/s0375-6505(99)00061-9

Appendix A

Sample ID	TDS (ppm)	pH@20 ˚C	SO_4 (ppm)	Cl (ppm)	CO_2 (ppm)	F (ppm)	Ca (ppm)	Na (ppm)	K (ppm)	Mg (ppm)	Fe (ppm)	Pb (ppm)	Zn (ppm)	Li (ppm)
OW 802	1740	9.6	125.3	1097.47	288.64	77.76	0.493	742.7	166	0.238	_	_	_	2.61
OW 803	1210	9.49	137.6	874.2	267.3	48.73	1.17	650.32	99.71	0.03	0.16	_	_	3.09
OW 805	2486	8.93	62.7	1239	367.6	102.1	0.163	1033	236	0.047	_	_	_	2.65
OW 52	4090	10.25	92.74	1576.8	143	141.31	0	1124.54	286.734	0	0.38	1.5596	5.1189	2.56
OW 52A	9730	10.05	322.96	3283.46	526.9	533.4	0	2630.63	197.14	0	0.24	2.0429	5.2323	3.06
OW 27,31,33	1030	8.74	28.3	463.04	46.2	53.4	0.175	445.9	44.72	0.004	_	_	4.3247	0.723
OW 32	1890	8.93	27.5	785.26	31.46	73.47	0.01	641.2	94.6	0.002	_	1.6934	4.2136	0.946
OW 35	3270	9.592	91.56	1785.56	230.12	233.24	0.116	1181	429.5	0.556	_	_	4.217	1.828
F4	36.2	4.39	8.04	4.69	579.7	0.15	2.4	1.34	0.2	0.2	0.1274	_	_	0.01
F5	14.3	4.41	5.07	5.33	260.7	0.04	0.41	1.6	0.25	0.06	0.397	_	_	0.01
HS 2	690	8.01	209.52	298.97	385	107.98	1.699	453.92	22.86	0.014	3.592	_	4.285	0.346